

Supporting information

Fabrication and potential applications of CaCO_3 /lentinan hybrid materials with hierarchical composite pores structure obtained by self-assembly of nanoparticles

Xiaoming Ma*, Shibao Yuan, Lin Yang*, Liping Li, Xiaoting Zhang, Yuanyuan Yang, Kui Wang

School of Chemistry and Chemical Engineering, Henan Normal University, Key Laboratory of Green Chemical Media and Reactions, Ministry of Education, Xinxiang 453007, P. R. China.

* To whom correspondence should be addressed. Tel: +86-373-3325058; Fax: +86-373-3328507.
e-mail: sunshinyma@hotmail.com

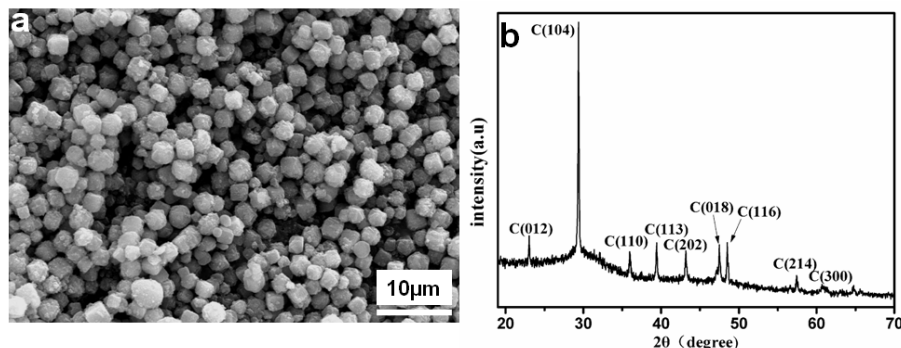


Fig. S1 SEM (a) and X-ray diffraction pattern (b) of CaCO_3 crystals obtained in the double-distilled water without lentinan. The X-ray diffraction (XRD) pattern indicated that the phase of the CaCO_3 was calcite (calcite JCPDS Card No. 05-0586) (Calcite peaks are marked with “C”).

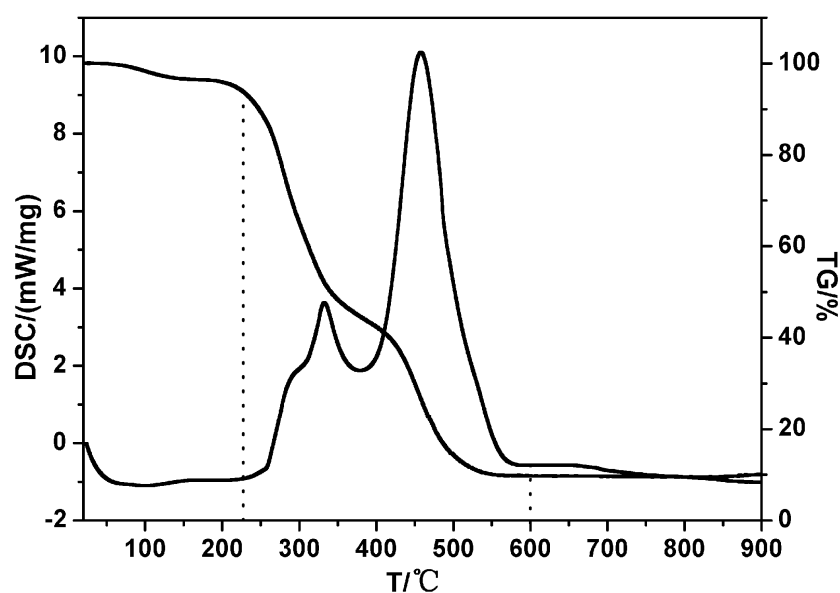


Fig. S2 TG-DTA curves of the pure lentinan.

Fig. S3 showed particle size distribution of intermediary species by dynamic light scattering from the solutions at 0 min (Fig.S3a) and 30min ((Fig.S3b) of crystallization, respectively. At a very early stage, e.g. 0 min, two species with around 4.7 nm, 36.4 nm were found, with the dominant species being the one with 4.7 nm. When growing for 30 min, two species with around 6.2 nm, 294.1 nm were found, with the dominant species being the one with 6.2 nm.

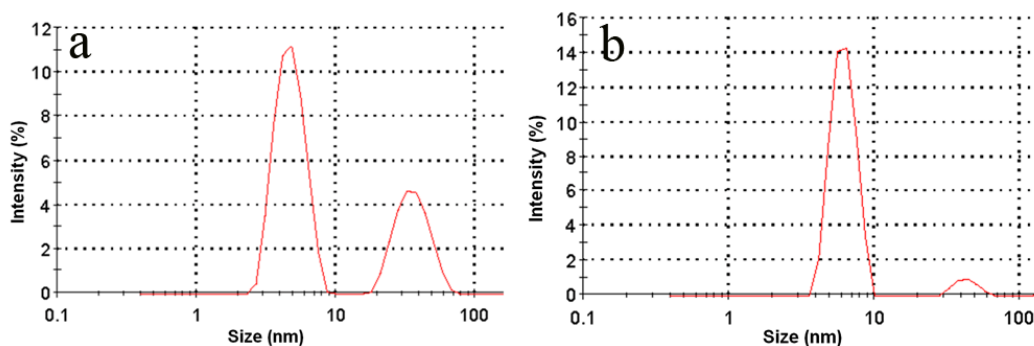


Fig. S3 Particle size distribution of intermediary species by dynamic light scattering from the solutions at 0 min (a) and 30min (b) of crystallization, respectively.

Using the autofluorescence of DOX, its loading content could be measured by UV-vis spectroscopy and the distribution of DOX into the HCPs CaCO_3 /lentinan microspheres was characterized by the confocal laser scanning microscopy (CLSM) (Fig. S4, supporting information). As shown in Fig. S4a, it can be observed that such types of plots present multilinearity, indicating that three loading steps (the fast adsorption or external surface adsorption stage, the gradual adsorption stage and the final equilibrium stage) take place in the process of loading DOX into the CaCO_3 microspheres. We suggest that there are possible reasons for these regions: DOX could facilely enter into the mesoporous pores on the HCPs CaCO_3 microspheres and the high initial DOX concentration is driving force of diffusion. And then the DOX was slowly loaded into the micropores in the wall of mesoporous.

The presence of DOX loaded inside the HCPs CaCO_3 /lentinan microspheres was further confirmed by using confocal laser scanning microscopy (Fig. S4b and c, supporting information). Fig. S4b and c show the CLSM images of the HCPs CaCO_3 /lentinan after 24 h of co-incubation with DOX under visible light and UV light, respectively. The interiors of the HCPs CaCO_3 microspheres exhibits strong fluorescent under UV light, which emits from the DOX molecules (DOX has two emission maxima wavelengths centered at 560 nm and 590 nm, respectively). The results indicates that DOX is indeed loaded inside the HCPs CaCO_3 /lentinan microspheres rather than simply adhered on the surface of CaCO_3 microspheres, and distributed homogeneously throughout the HCPs CaCO_3 /lentinan microspheres. Further TEM observation shows the dark shadows at the centers of the HCPs CaCO_3 /lentinan-DOX microspheres reveal again the successful loading (Fig. S5, supporting information).

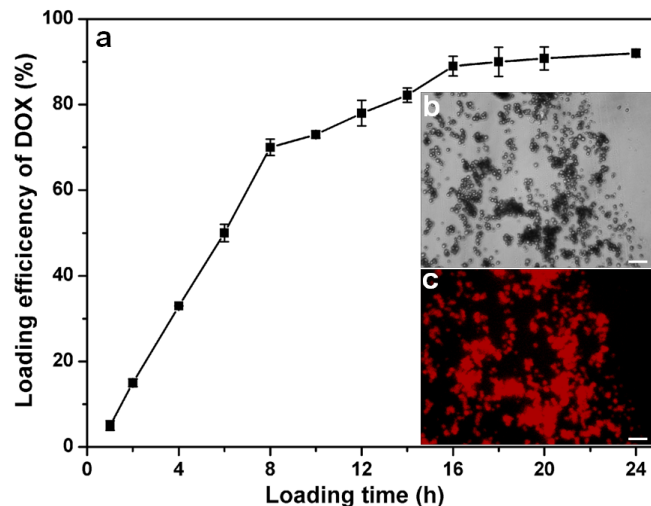


Fig. S4 (a) Loading kinetics of DOX into the HCPs CaCO_3 /lentinan hybrid materials. (b and c) CLSM images for the HCPs CaCO_3 /lentinan-DOX under visible light and UV light, respectively.
(Scale bar: 20 μm)

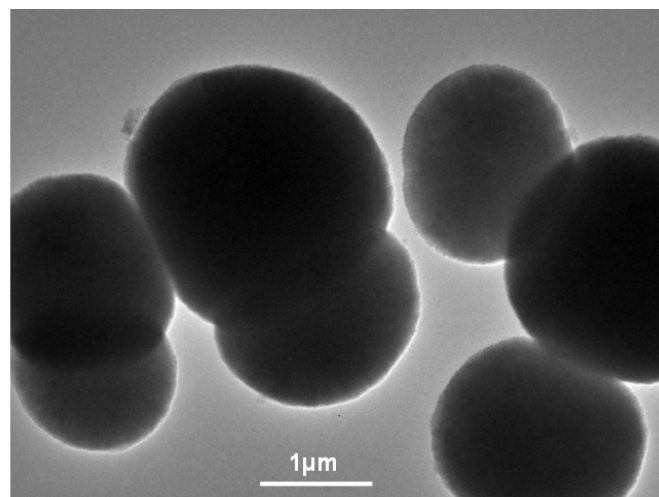


Fig. S5 TEM images of CaCO_3 /lentinan microspheres after DOX loading.

The Langmuir equation is expressed as follows¹:

$$q_e = \frac{q_{\max} K_L C_e}{1 + K_L C_e} \quad (1)$$

where C_e is the equilibrium concentration of CR in solution (mg/L), q_e is the equilibrium adsorption capacity of CR on the adsorbent (mg/g), q_{\max} is the maximum adsorption capacity of

the adsorbent corresponding to complete monolayer coverage on the surface (mg/g), and K_L is the Langmuir adsorption constant (L/mg) and related to the free energy of adsorption. Eq. 1 can be rearranged to a linear form:

$$\frac{C_e}{q_e} = \frac{1}{q_{\max} K_L} + \frac{C_e}{q_{\max}} \quad (2)$$

The constants q_{\max} and K_L can be calculated from the intercepts and the slopes of the linear plots of C_e/q_e versus C_e .

The essential characteristics of the Langmuir equation can be expressed in term of a dimensionless separation factor, R_L , defined as follows²:

$$R_L = \frac{1}{1 + K_L C_0} \quad (3)$$

where C_0 is the highest initial solute concentration and K_L is the Langmuir's adsorption constant (L/mg).

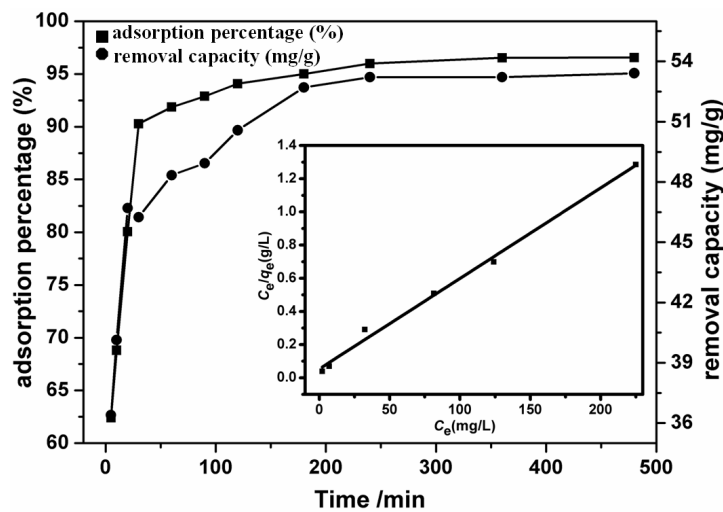


Fig. S6 The variation of adsorption capacity and adsorption percentage for CR with adsorption time on the HCPs CaCO_3 /lentinan hybrid materials ($T = 25^\circ\text{C}$ adsorbent dose = 428 mg/L; CR concentration = 25 mg/L and pH=7). The inset is the Langmuir isotherms for CR adsorption onto the HCPs CaCO_3 /lentinan hybrid materials at 25°C .

The Freundlich equation is an empirical equation and can be written as follows³:

$$q_e = K_F C_e^{1/n} \quad (4)$$

where q_e is the solid phase adsorbate concentration in equilibrium (mg/g), C_e the equilibrium liquid phase concentration (mg/L), K_F the Freundlich constant (mg/g)(L/mg) $^{1/n}$ and $1/n$ is the heterogeneity factor. A linear form of the Freundlich expression can be obtained by taking logarithms of Eq. (4):

$$\ln q_e = \ln K_F + \frac{1}{n} \ln C_e \quad (5)$$

Therefore, a plot of $\ln q_e$ versus $\ln C_e$ (Fig. S7) enables the constant K_F and exponent $1/n$ to be determined.

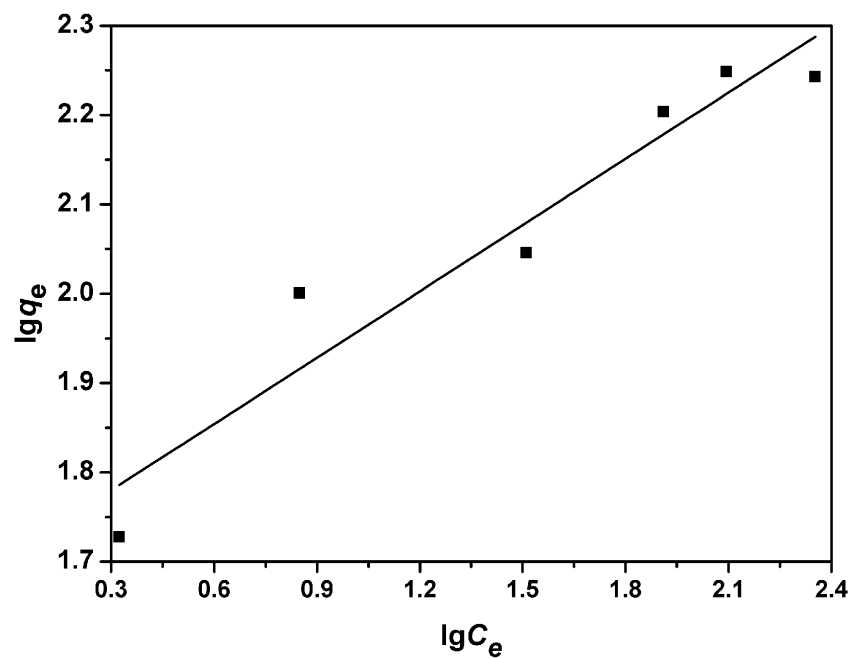


Fig. S7. Freundlich isotherm for CR adsorption onto the hierarchical composite pores CaCO₃ at 25 °C.

Table S1 Langmuir and Freundlich model parameters of the hierarchical composite pores CaCO_3

sample	Langmuir constants				Freundlich constants		
	q_{\max} (mg/g)	K_L (L/mg)	R^2	R_L	$K_F(\text{mg/g})$ $(\text{L/mg})^{1/n}$	n	R^2
the hierarchical composite pores CaCO_3	213.2	0.11	0.99	0.029	50.8	4.1	0.88

1 I. Langmuir, *J. Am. Chem. Soc.*, 1918, **40**, 1361.

2 K.R. Hall, L.C. Eagleton, A. Acrivos and T. Vermeulen, *Ind. Eng. Chem. Fundam.*, 1966, **5**, 212.

3 H. M. F. Freundlich, *J. Phys. Chem.* 1906, **57**, 385.